Continuous Heating Transformation (CHT) Cure Diagram of an Aromatic Amine/Epoxy System at Constant Heating Rates

GUY WISANRAKKIT and JOHN K. GILLHAM*

Polymer Materials Program, Department of Chemical Engineering, Princeton University, Princeton, New Jersey 08544

SYNOPSIS

The overall reaction kinetics of a high-T_g tetrafunctional aromatic diamine/difunctional epoxy system (maximum glass transition temperature, $T_{g\infty}$ = 182°C), which can satisfactorily describe the rate of the reaction in both kinetically and diffusion-controlled regimes, had been determined earlier from isothermal conversion/T_g data by differential scanning calorimetry (DSC). The mathematical expression of the kinetics, together with the unique one-to-one relationship between T_g and chemical conversion, is used to calculate the material's T_g vs. time under heating at constant rates. For a heating scan from below T_{g0} (the glass transition temperature of the unreacted material), initial devitrification corresponds to the reaction temperature (T_{cure}) first passing through the T_g of the reacting material; vitrification corresponds to T_g becoming equal to the increasing T_{cure} after initial devitrification; and finally, upper devitrification corresponds to T_g eventually falling below the rising T_{cure}. The results of the calculation correlate well with the available experimental data of the dynamic mechanical behavior of the material during temperature scans at constant rates that were obtained by the torsional braid analysis (TBA) technique. T_g is calculated to remain slightly higher than T_{cure} after vitrification due to the influence of diffusion control, the difference being greater for lower heating rates. The limiting heating rate with no initial devitrification and that with no vitrification are also calculated.

INTRODUCTION

During cure of a liquid thermosetting system at an isothermal temperature (T_{cure}), the glass transition temperature (T_g) of the material increases with chemical conversion, a process that can transform the material from liquid to glass. The reaction is predominantly kinetically controlled in the fluid region (i.e., $T_g < T_{cure}$); diffusion control becomes a significant factor after the material vitrifies (i.e., $T_g > T_{cure}$) due to the relatively low submolecular mobilities of functional groups in the glass transition region.[1-6] A recent study[7,8] from our laboratory on a stoichiometric mixture of a tetrafunctional aromatic diamine/diepoxy system successfully resulted in a rate expression for the reaction kinetics, which is applicable throughout the entire range of cure in both the chemical and diffusion-controlled regimes. The study also demonstrated that there is a unique one-to-one relationship between T_g and conversion independent of different time-temperature cure paths. The assumed reaction kinetics for this amine/epoxy system has been further tested with both excess epoxy and excess amine off-stoichiometric ratio systems.[9]

The derived reaction kinetics, together with the relationship between T_g and conversion, was used[7-9] to calculate the entire vitrification curve and a series of iso-T_g contours (in the regions both before and after vitrification) in the isothermal time-temperature-transformation (TTT) cure diagram for the system. The diagram, schematically shown in Figure 1,[10-12] plots the cure temperatures vs. the times to reach different events that the material encounters during isothermal cure: molecular gelation (corresponding to the incipient formation of infinite molecules), vitrification (corresponding to T_g increasing to T_{cure} due to chemical reaction), iso-T_g (corresponding to T_g rising to a specified value),

* To whom correspondence should be addressed.

Journal of Applied Polymer Science, Vol. 42, 2453–2463 (1991)
 CCC 0021-8995/91/092453-11$04.00

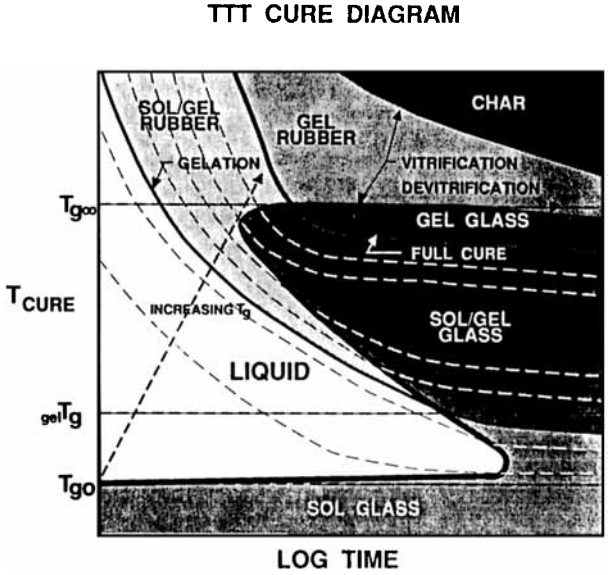

Figure 1 A generalized isothermal time-temperature-transformation (TTT) cure diagram for a thermosetting system, showing three critical temperatures (i.e., T_{g0}, $T_{g\infty}$, and $_{gel}T_g$), states of the material, and contours characterizing the setting and degradation processes. The full cure contour corresponds to $T_g = T_{g\infty}$. Molecular gelation corresponds to $T_g = {}_{gel}T_g$. Other iso-T_g contours are included (dashed curves).

devitrification (corresponding to T_g decreasing to T_{cure} due to chemical degradation), and char formation (corresponding to T_g increasing to T_{cure} at high temperatures due to thermal degradation).

Under nonisothermal cure conditions, the material can also encounter various events similar to the isothermal case. Analogous to the isothermal TTT cure diagram is the continuous heating transformation (CHT) cure diagram that displays the times and temperatures required to reach these events during the course of continuous heating at different constant heating rates.[12-14]

This paper examines the behavior of the aromatic diamine/diepoxy system, used in the earlier study, under continuous heating conditions. The progress of the material's T_g during the temperature scans was calculated from the reaction kinetics and the empirical relationship between T_g and conversion. The knowledge of the behavior of the material's T_g at different heating rates permits calculation of a theoretical initial devitrification/vitrification/upper vitrification contour in the CHT diagram for the material, which can then be compared with data determined from torsional braid analysis (TBA) experiments. This study provides an additional means for checking the validity of the assumed kinetics when the material is subjected to nonisothermal constant heating conditions. A preliminary report has been published.[15]

CHEMICAL REACTANTS

The material chosen for this study is a liquid difunctional epoxy (diglycidyl ether of bisphenol A, DER 332, Dow Chemical Co., epoxy equivalent weight = 174 g/eq) cured with a stoichiometric amount of a crystalline (melting range = 125–128°C) tetrafunctional aromatic diamine (trimethylene glycol di-*p*-aminobenzoate, TMAB, Polaroid Corp., amine equivalent weight = 157 g/eq). The chemical structures of both reactants are shown in Figure 2. A mixture of the two reactants was accomplished by dissolving the crystalline amine in the liquid epoxy at 100°C with vigorous stirring for 15 min to ensure homogeneous mixing. The warm clear viscous mixture was subsequently degassed for 20 min in a vacuum oven held at room temperature and poured into numerous small aluminum weighing pans, which were then individually placed in plastic bags, placed inside a dessicator, and stored in a freezer.

For purposes of consistency, the same master batch of the mixture that has been used for the previous study of the isothermal cure kinetics using differential scanning calorimetry (DSC)[7,8] was used for the present study of the material's behavior under constant heating rates using TBA.

EXPERIMENTAL

A torsional braid analyzer[10,12] equipped with a temperature programmer/controller was used to monitor the dynamic mechanical behavior of the material (~ 1 Hz) during cure under continuous heating at various heating rates. Before an experiment, an aluminum pan containing the reactive mixture inside its plastic bag was removed from the freezer and left at room temperature for at least 20 min before being taken out of the plastic bag. The viscous reactive liquid was then coated on a glass braid (ca. 50 mm in length) to form a specimen in the TBA experiment. Excess material on the braid was removed by squeezing the impregnated glass braid between aluminum foil. The final amount of the material on each braid was approximately 10–15 mg. The specimen, mounted between two vertical rods (parts of the inner TBA pendulum assembly), was inserted into the TBA temperature chamber at 30°C under a continuously flowing He atmosphere and then quenched at a programmed rate of 10°C/min to

CHEMICAL REACTANTS

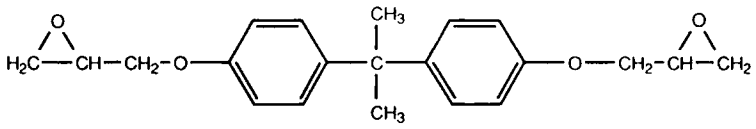

Diglycidyl Ether of Bis-phenol A (DER332, Dow Chemical Co.)

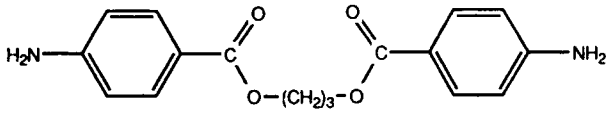

Trimethylene glycol di-p-aminobenzoate (TMAB, Polaroid Corp.)

REACTIONS

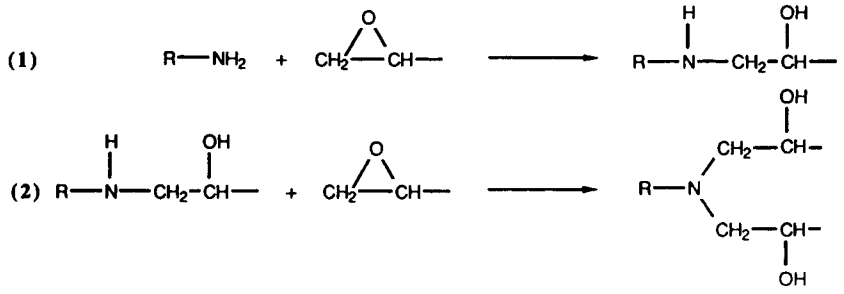

Figure 2 Chemical reactants and chemical reactions.

−50°C. After the temperature was in control at −50°C, the specimen was heated from −50°C to 250°C at a preprogrammed heating rate. Two dynamic mechanical material properties, namely, relative rigidity and logarithmic decrement, were monitored and recorded during the temperature ramp from −50 to 250°C. After the temperature had reached 250°C, the specimen was subjected to the final temperature scans, 250 → −180 → 250°C, while its dynamic mechanical properties were also monitored (data not shown in this report). Experiments were performed at heating rates ranging from 0.03 to 1°C/min.

The automated TBA torsion pendulum system was manufactured by Plastics Analysis Instruments, Inc., Princeton, NJ.

RESULTS AND DISCUSSION

Behavior during Temperature Scans

Figure 3 shows the TBA relative rigidity of the material during a series of temperature scans from −50 to 250°C at constant heating rates (0.03, 0.06, 0.09, 0.12, 0.16, 0.19, 0.31, and 0.46°C/min). The corresponding logarithmic decrement data are shown in Figure 4. Various events that the specimen encounters during the course of a temperature scan can be assigned from the successive maxima in the peaks of the logarithmic decrement spectrum. For a temperature scan starting below the glass transition temperature of the initially unreacted material (T_{g0}), these events[12-14] can include initial devitrification (corresponding to the first softening of the initial glassy reactive mixture), several undesignated events, macroscopic gelation (probably an isoviscous event),[10,16] vitrification (corresponding to T_g rising to the cure temperature), upper devitrification at high temperatures (corresponding to T_g decreasing to the increasing cure temperature), and thermal degradation at high temperatures. Some of the logarithmic decrement spectra in Figure 4 show (in the order of increasing temperature) initial devitrification, two or three undesignated events, macroscopic gelation, vitrification, and upper devitrifica-

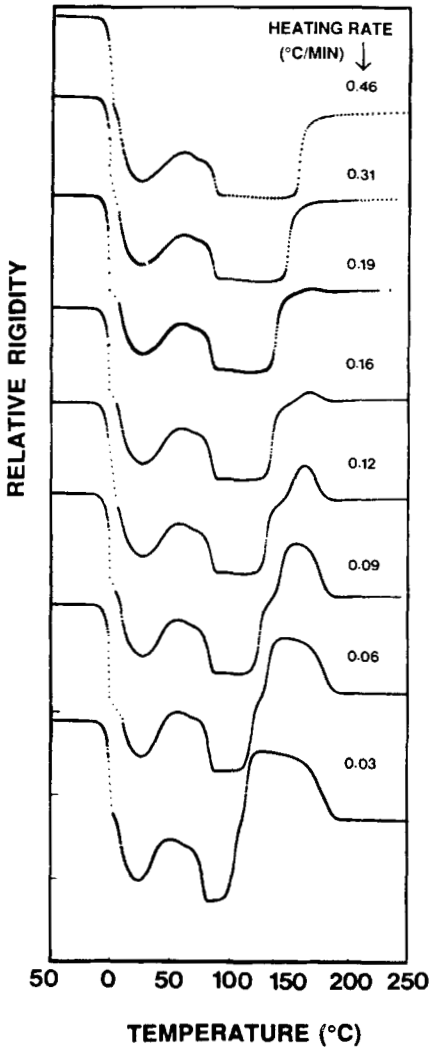

Figure 3 TBA relative rigidity ($1/P^2$) of DER 332/TMAB during continuous heating from −50 to 250°C at different heating rates.

tion (see, e.g., the marked spectrum at 0.09°C/min). These results at different heating rates can be summarized in the form of an experimental CHT diagram, in which the temperature vs. log(time) to reach an event at a given heating rate is displayed, as shown in Figure 5. In the following section, calculations are performed to determine quantitatively the times and temperatures to reach initial devitrification, vitrification, and upper devitrifcation at different heating rates, employing the kinetic model derived in the earlier study[7,8] for this amine/epoxy system and the empirical T_g vs. conversion relationship; the results are then compared with the experimental data in Figure 5.

Kinetic Model for the Amine/Epoxy Reaction

Differential scanning calorimetry (DSC) has been used to study the chemical kinetics of this amine/epoxy system under isothermal cure conditions. The results of the study are available elsewhere.[7,8] The main conclusions relavant to the present study are summarized in this section.

The chemical kinetics of the reaction between the epoxy and amine is satisfactorily described by a sec-

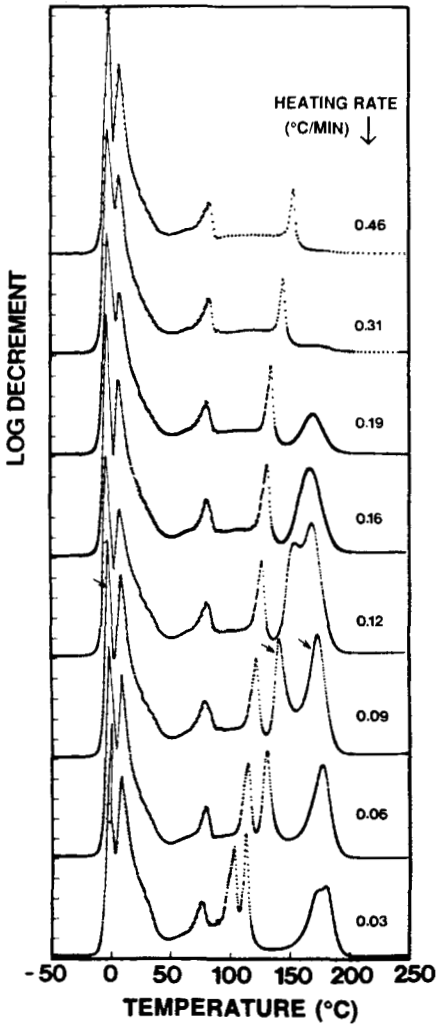

Figure 4 TBA logarithmic decrement of DER 332/TMAB during continuous heating from −50 to 250°C at different heating rates. Different events are identified from the maxima of the peaks of each spectrum. The events relevant to this work are initial devitrification, vitrification, and upper devitrification, which are identified as the first, fifth, and sixth peaks in order of increasing temperature, respectively, for the marked spectrum at 0.09°C/min.

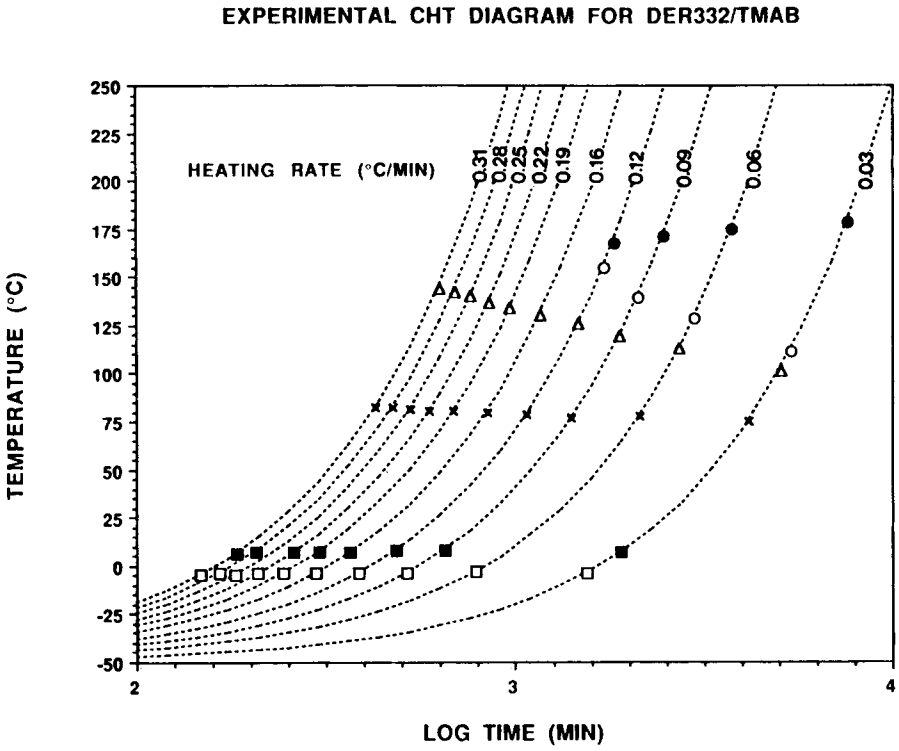

Figure 5 Events encountered during continuous heating at constant rates summarized in the form of an experimental CHT diagram: (□) initial devitrification, (■ and x) two undesignated events, (Δ) macroscopic gelation, (○) vitrification, and (●) devitrification.

ond-order reaction mechanism autocatalyzed by hydroxyl groups[17] with equal reactivity for all amino hydrogens. The reaction is shown to be predominantly kinetically controlled up to isothermal vitrification. After vitrification, the influence of diffusion control becomes apparent and eventually dominates the reaction. The time scale for the rate of reaction is a sum of the time for diffusion of functional groups and the time for chemical reaction. When a reaction is diffusion controlled, the diffusion of chemical reactants becomes the limiting step. The effect of diffusion control can be incorporated into the reaction kinetics by modifying the overall reaction rate constant. During the course of cure, the overall rate constant is assumed to be a combination in parallel of the chemical rate constant and the diffusion rate constant.[18] The latter is governed by the relaxation of submolecular chain segments of the polymer. The temperature dependence of the kinetically controlled rate constant is given by the usual Arrhenius-type expression, whereas that of the diffusion-controlled rate constant is assumed to be given by a modified form of the WLF equation, in which the temperature dependence is governed by $T_{cure} - T_g$.[19,20] Calculations using these modified rate constants have been shown to provide good correlation with experimental isothermal T_g and conversion versus time data in both chemical and diffusion controlled regimes.[7,8]

The mathematical expression of the aforementioned kinetic model for the present amine/epoxy system can be summarized as follows[7,8]:

$$\frac{dx}{dt} = k_a(1 - x)^2(x + 0.05548) \tag{1}$$

where x is the fractional conversion and k_a is the overall rate constant;

$$\frac{1}{k_a} = \frac{1}{k_T} + \frac{1}{k_d} \tag{2}$$

where k_T is the rate constant for kinetic control and k_d is the rate constant for diffusion control:

$$k_T = A_0 \exp\left(-\frac{E}{RT}\right) \tag{3}$$

where E = 15.2 Kcal/mol, and $A_0 = 7.68 \times 10^6$ min^{-1}, and

$$k_d = 30.64 \exp\left\{\frac{42.61\ (T - T_g)}{51.6 + |T - T_g|}\right\} \qquad (4)$$

The value of k_T is a constant at an isothermal temperature, whereas that of k_d varies with both cure temperature and conversion (T_g). Equations (1)–(4) describe the conversion of the material as a function of time, temperature, and T_g. The same study[7,8] also showed that T_g relates to conversion in a unique one-to-one fashion independent of cure path. Therefore, using the relationship between T_g and conversion for this chemical system, eqs. (1)–(4) can completely describe the progress of the chemical reaction in terms of T_g, given the initial conversion of the material, for all isothermal and nonisothermal cure paths.

T_g vs. Conversion

The TBA technique was used to determine the T_g of the present amine/epoxy material with different extents of chemical conversion. The material, impregnated on TBA braids, was cured inside the TBA instrument at different isothermal temperatures for different times, then cooled at 1°C/min to −180°C. The T_g of each specimen was determined during the subsequent temperature scan from −180 to 250°C at 1°C/min as the maximum in the logarithmic decrement peak of the glass transition. The fractional conversion of each specimen was determined from the DSC kinetic calculation[7,8] for the material with exactly the same cure history (in both the isothermal and temperature scanning conditions). The plot of the experimental TBA T_g vs. the corresponding fractional conversion is shown in Figure 6. Different symbols represent different cure temperatures. It can be clearly seen that there is a unique one-to-one relationship between T_g and conversion independent of the time-temperature path of cure. The solid line represents the best-fit calculation of the data to the DiBenedetto equation[3,21,22]:

$$\frac{T_g - T_{g0}}{T_{g0}} = \frac{(E_x/E_m - F_x/F_m)x}{1 - (1 - F_x/F_m)x} \qquad (5)$$

where T_g and T_{g0} are in degrees Kelvin. T_{g0} for this system determined by TBA is −3°C (270 K). The

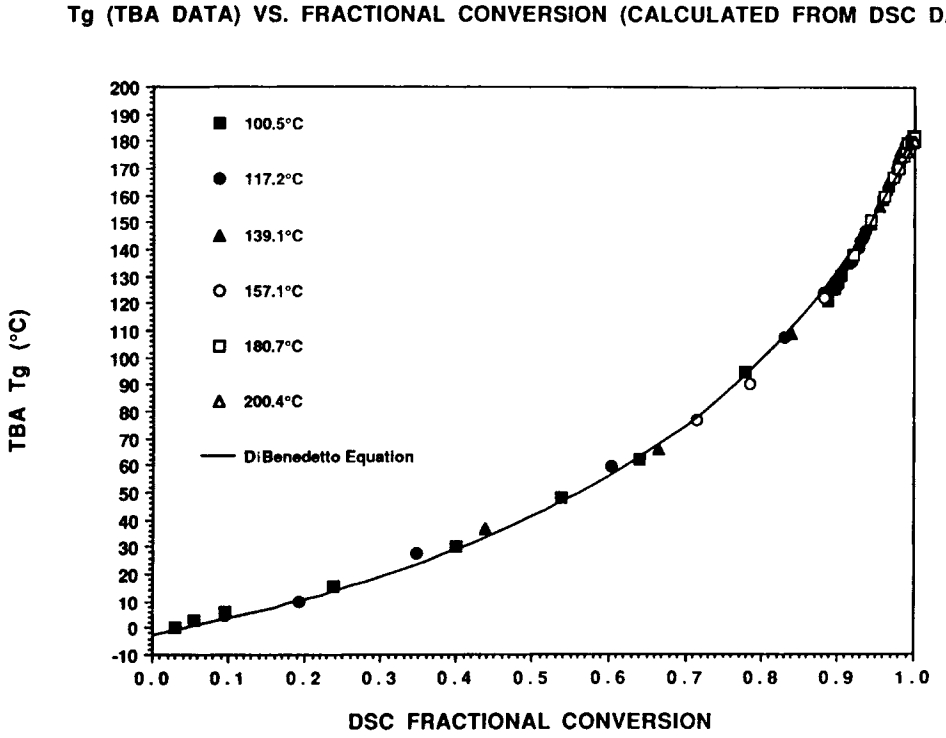

Figure 6 The unique one-to-one relationship between TBA T_g and fractional conversion for DER 332/TMAB. Different symbols represent material cured at different temperatures. The solid curve represents the best-fit calculation from the DiBenedetto equation (eq. 5).

best-fit values for the two ratios, E_x/E_m (the ratio of lattice energies for crosslinked and uncrosslinked polymers) and F_x/F_m (the corresponding ratio of segmental mobilities), are determined to be 0.52 and 0.31, respectively. Equation (5) provides a reasonable semiempirical relationship in an analytical form that can be applied to relate TBA T_g values to conversion in the following calculation of the CHT diagram.

CHT Diagram Calculation: Initial Devitrification, Vitrification, and Upper Devitrification

In a CHT experiment, a TBA specimen is heated from −50 to 250°C at a constant heating rate, r (°C/min). The procedure for calculating the times to the different transitions (i.e., initial devitrification, vitrification, and upper devitrification) is as follows: For a constant heating rate, r, the progress of chemical reaction as a function of cure time, t, can be calculated from eqs. (1)-(4) by substituting $T = T_i + rt$, where $T_i = -50$°C is the starting temperature of the experiment. The fractional conversion, x, vs. time can then be converted into T_g vs. time by employing the DiBenedetto relationship, eq. (5). Therefore, given a heating rate, r, eqs. (1)-(5) can completely describe how the T_g of the material increases as a function of time.

Figure 7 shows the calculated T_g vs. log(time) at different heating rates (solid curves) together with the corresponding cure temperature vs. log(time) (short-dashed curves). The initial devitrification, vitrification, and upper devitrification events are identified for each heating rate as the first, second, and third intersections (in time and temperature) of the T_g and cure temperature curves. The S-shaped contour (long-dashed curve) in Figure 7 represents the theoretical locus of all initial devitrification (the lower section of the S), vitrification (the middle section of the S), and upper devitrification (the upper section of the S) events at different heating rates.

Since heating starts at a temperature below T_{g0}, the initial uncured specimen is almost in the glassy state. Initial devitrification (the first softening

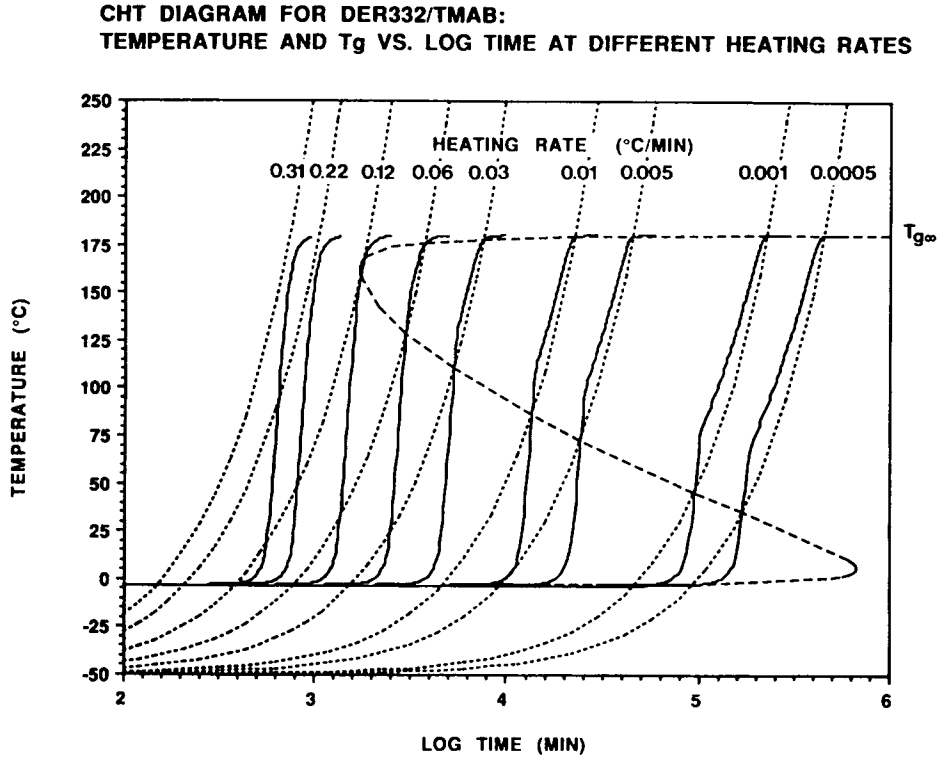

Figure 7 Calculations of the increase of T_g vs. log(time) under continuous heating at different rates (solid curves). Initial devitrification, vitrification, and upper devitrification events are quantitatively determined from the intersections between these T_g curves and the heating curves (short-dashed curves). The S-shaped long-dashed contour represents the initial devitrification-vitrification-upper devitrification CHT envelope.

point) is encountered when the cure temperature first passes through the glass transition temperature of the reacting material. It can be seen from Figure 7 that, for a high heating rate, the initial devitrification generally occurs at T_{g0} because the short time interval during heating to T_{g0} is not sufficient to allow substantial reaction to raise the T_g of the material above T_{g0}. For a very low heating rate, however, this event can occur at temperatures higher than T_{g0}, since by the time the temperature rises to T_{g0}, a substantial extent of reaction has advanced the T_g of the material above T_{g0}; consequently, the material does not devitrify at T_{g0}.

At a low limiting heating rate of 8.2×10^{-5}°C/min (0.8°C/week), initial devitrification and vitrification for this particular system occur simultaneously. For heating rates lower than this limiting heating rate, no initial devitrification is encountered. In these cases, the reaction proceeds in the glass transition region without liquifying, i.e., polymerization occurs under conditions of maximum density, and devitrification only occurs near or at $T_{g\infty}$. A practical implication of such a cure path (to a temperative short of $T_{g\infty}$) is that the material will develop less internal stresses since no change of state is encountered during cure. Analogous to this low limiting heating rate is a high limiting rate of 0.13°C/min at which the vitrification and the upper devitrification events occur simultaneously. Above initial devitrification, for heating rates greater than 0.13°C/min, the T_g of the material never reaches the cure temperature. Thus, for these cases, the reaction proceeds to completion entirely in the liquid and rubbery states without encountering vitrification and devitrification. Such a cure condition is often necessary for rapid molding operations.

For heating rates in the range between these two limiting rates (8.2×10^{-5}°C/min $< r <$ 0.13°C/min), after the occurrence of initial devitrification, the material is in the liquid or rubbery states ($T_g < T_{cure}$) and reaction in the early stages can proceed in such a way that the T_g of the material can rise faster than the cure temperature. The point at which T_g rises to the increasing T_{cure} is identified as vitrification ($T_g = T_{cure}$). Beyond vitrification, the material is in the glass transition region ($T_{cure} < T_g < T_{cure} + 50$), in which the reaction rate is drastically reduced due to diffusion control of the available chemical reactive sites; T_g remains slightly above T_{cure} with greater differences at a lower heating rates.

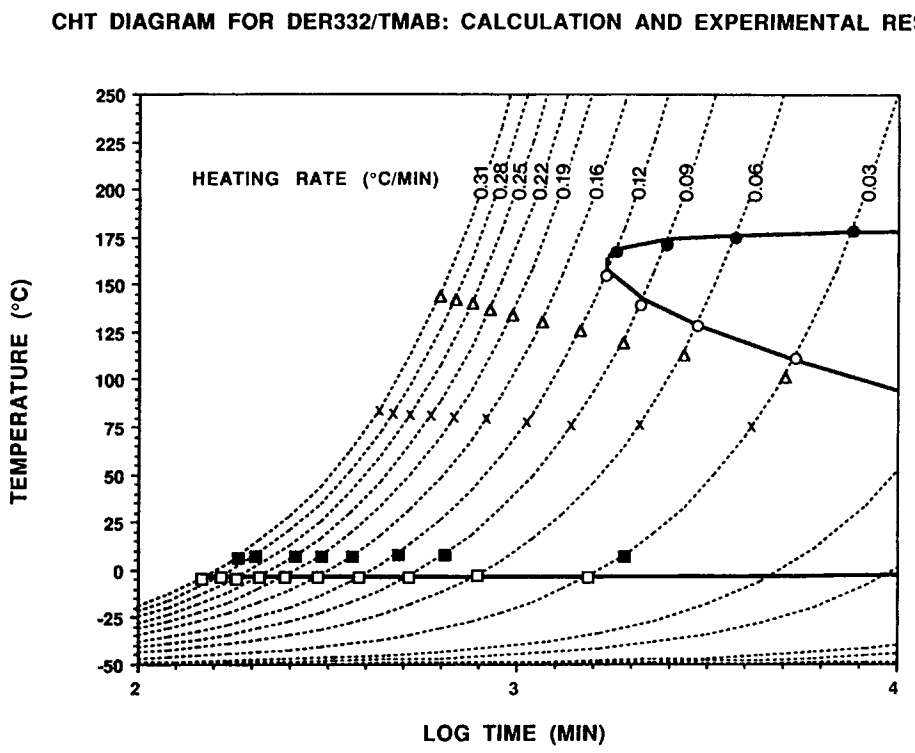

Figure 8 Comparison of the calculated initial devitrification-vitrification-upper devitrification CHT envelope from Figure 7 (solid curve) with the available experimental data from Figure 5 (symbols).

The magnitude of $T_g - T_{cure}$ increases after vitrification before gradually decreasing as the reaction proceeds toward high temperatures, due to depletion of chemical reactants. Eventually, upper devitrification occurs when the T_g of the material falls below the increasing cure temperature, after which the reaction proceeds to completion in the rubbery state ($T_g < T_{cure}$), if the reaction had not been completed before devitrification.

Figure 8 compares the calculated S-shaped (initial devitrification-vitrification-upper devitrification) envelope of the CHT diagram with the available TBA experimental data for heating rates ≥ 0.03°C/min. It is apparent that there is a good correlation between the calculation results and the experimetnal data. The agreement provides support for the validity of the assumed kinetic model.

In a previous work from this laboratory,[13] a simple methodology was presented for calculating the initial devitrification-vitrification-upper devitrification envelope in the CHT diagram when information on the diffusion-controlled kinetics is not readily available. The method assumes in a continuous heating case that the reaction is only kinetically controlled up to vitrification, and that beyond vitrification, the T_g of the material increases at the same rate as does the heating temperature as long as the additional conversion with each small temperature increment is sufficient to increase T_g to T_{cure}. Upper devitrification occurs only when the reaction rate is not sufficient to keep $T_g = T_{cure}$ because of high conversion at high temperatures or because of the relatively high rate of temperature increase. Calculations are also performed for the current system according to the above assumptions, i.e., that the reaction is only kinetically controlled prior to vitrification [eqs. (1)–(3) where $k_a = k_T$] and the reaction proceeds along the $T_g = T_{cure}$ path after vitrification. The resulting CHT diagram is shown in Figure 9 as a heavily dashed S-shape contour superimposed over the previously calculated diagram (using the more complete kinetics with diffusion control) from Figure 7 (shown as a solid S-shaped contour), together with the available experimental data (symbols).

It can be seen from Figure 9 that the approximate

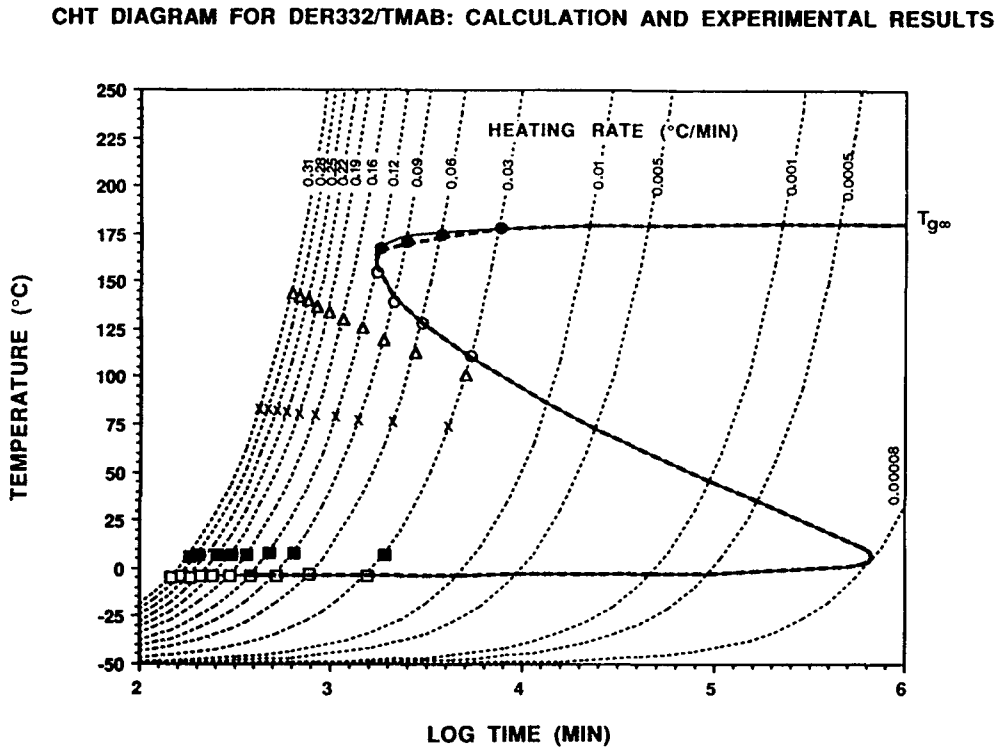

Figure 9 Comparison of the calculated CHT diagram using complete kinetics (solid S-shaped contour) with the less rigorous calculation assuming that T_g follows T_{cure} after vitrification (dashed S-shaped contour). TBA experimental data are also included as symbols (see the legend for each symbol in Fig. 5).

calculation provides reasonable agreement with the experimental data. This is because the assumptions closely approximate the real behavior of the material: (a) The effect of diffusion control has been shown to be significant only after vitrification (when $T_g \geq T_{cure}$).[7,8] Consequently, the assumption that the reaction is only kinetically controlled prior to vitrification is, in fact, properly applicable. (b) After vitrification, in the actual continuous heating situation, the value of T_g remains a few degrees above T_{cure}. However, diffusion control decreases the rate of increase of T_g to approximately the same as that of the heating rate (see Fig. 7). Therefore, the second assumption that T_g follows T_{cure} after vitrification can be considered to be a reasonable approximation to the material's actual behavior. The approximate calculation yields values of the upper devitrification points a few degrees lower than the actual case since the actual T_g is higher than the assumed T_g in the calculation. This is apparent at high heating rates (see Fig. 9); for low heating rates, both calculations yield values for the upper devitrification very close to $T_{g\infty}$, results which, therefore, are indistinguishable.

CONCLUSIONS

1. The kinetics of the reaction of an aromatic amine/epoxy system and the unique one-to-one relationship between T_g and conversion are used as a basis for modeling the increase of T_g under continuous heating at different heating rates. Initial devitrification, vitrification, and upper devitrification events at a constant heating rate are quantitatively determined from the intersections between T_g and T_{cure} vs. time curves. The results of the calculation correlate well with the dynamic mechanical behavior of the material determined by the TBA technique during temperature scans at constant rates.
2. The calculation shows that initial devitrification is generally encountered at the glass transition temperature of the unreacted material (T_{g0}) except at very low heating rates, for which the initial devitrification occurs at $T > T_{g0}$.
3. Prior to vitrification ($T_g < T_{cure}$), the reaction is kinetically controlled. After vitrification, T_g rises a few degrees above the cure temperature before the effect of diffusion control becomes significant and limits the rate of increase of T_g. Consequently, the magnitude of $T_g - T_{cure}$ increases initially after vitrification and then decreases gradually as the reaction proceeds at higher conversions at higher temperatures. Eventually, upper devitrification occurs when T_g falls below T_{cure}.
4. A limiting calculation of the CHT diagram which assumes that the reaction is only kinetically controlled before vitrification and that T_g follows T_{cure} after vitrification, provides a reasonable approximation to the actual material's behavior on heating.
5. The agreement between the theoretical calculation of the CHT envelope and the experimental data supports the validity of the assumed reaction kinetics and of the empirical one-to-one relationship between T_g and conversion.

This research was supported in part by the Office of Naval Research.

REFERENCES

1. G. Wisanrakkit and J. K. Gillham, in *Polymer Characterization,* T. Provder and C. Craver, Eds., Am. Chem. Soc. Adv. Chem. Ser. No. 227, American Chemical Society, Washington, DC, 1990.
2. K. P. Pang and J. K. Gillham, *J. Appl. Polym. Sci.,* **37,** 1969 (1989).
3. J. B. Enns and J. K. Gillham, *J. Appl. Polym. Sci.,* **28,** 2567 (1983).
4. I. Mita and K. Horie, *J. Macromol. Sci. Rev. Macromol. Chem. Phys.,* **C27**(1), 91 (1987).
5. I.-C. Choy and D. J. Plazek, *J. Polym. Sci. B Polym. Phys.,* **24,** 1303 (1986).
6. S. Lunak, J. Vladyka, and K. Dusek, *Polymer,* **19,** 931 (1978).
7. G. Wisanrakkit, Ph.D. Dissertation, Department of Chemical Engineering, Princeton University, Princeton, NJ, 1990.
8. G. Wisanrakkit and J. K. Gillham, *J. Coat. Tech.,* **62** (783), 35–50 (1990); *J. Appl. Polym. Sci.,* **41,** 2885 (1990).
9. S. L. Simon, G. Wisanrakkit, and J. K. Gillham, *Am. Chem. Soc. Prepr. Div. Polym. Mat. Sci. Eng.,* **61,** 799 (1989).
10. J. K. Gillham, in *Developments in Polymer Characterisation-3,* Dawkins, J. V. Ed., Applied Science Publishers, London, UK, 1982, Chap. 5.
11. J. K. Gillham, *Polym. Eng. Sci.,* **19,** 670 (1979); Ibid., **26**(20), 1429 (1986).
12. J. B. Enns and J. K. Gillham, in *Polymer Characterization,* Am. Chem. Soc. Adv. Chem. Ser. No. 203,

Craver, C. D., Ed., American Chemical Society, Washington, DC, 1983, pp. 27–63.
13. G. Wisanrakkit, J. K. Gillham, and J. B. Enns, *J. Appl. Polym. Sci.*, **41,** 1895 (1990).
14. L. C. Chan, H. N. Naé, and J. K. Gillham, *J. Appl. Polym. Sci.*, **29,** 3307 (1984).
15. G. Wisanrakkit and J. K. Gillham, *Am. Chem. Soc. Prepr. Div. Polym. Chem.*, **31**(1), 293 (1990).
16. H. Stutz and J. Mertes, *J. Appl. Polym. Sci.*, **38,** 781 (1989).
17. K. Horie, H. Hiura, M. Sawada, I. Mita, and H. Kambe, *J. Polym. Sci. A-1,* **8,** 1357 (1970).
18. I. Havlicek and K. Dusek, in *Crosslinked Epoxies,* Sedlacek, B. and Kahovec, J., Eds., Walter de Gruyter, Berlin, 1987, pp. 417–424.
19. M. L. Williams, R. F. Landel, and J. D. Ferry, *J. Am. Chem. Soc.*, **77,** 3701 (1955).
20. D. H. Kaelble, *Computer Aided Design and Manufacture,* Marcel Dekker, New York, 1985, Chap. 4, pp. 113–148.
21. A. T. DiBenedetto and L. E. Nielsen, *J. Macromol. Sci. Rev. Macromol. Chem.*, **C3**(1), 69 (1969).
22. H. E. Adabbo and R. J. J. Williams, *J. Appl. Polym. Sci.*, **27,** 1327 (1982).

Received December 6, 1989
Accepted August 2, 1990